



OPEN

Observation of Wave Packet Distortion during a Negative-Group-Velocity Transmission

SUBJECT AREAS:

ULTRAFAST PHOTONICS

CONDENSED-MATTER PHYSICS

Received

7 July 2014

Accepted

6 January 2015

Published

29 January 2015

Correspondence and requests for materials should be addressed to L.R. (ranlx@zju.edu.cn)

* These authors contributed equally to this work.

Dexin Ye^{1*}, Yannick Salamin^{1,5*}, Jiangtao Huangfu¹, Shan Qiao², Guoan Zheng^{3,4} & Lixin Ran¹

¹Laboratory of Applied Research on Electromagnetics (ARE), Zhejiang University, Hangzhou 310027, China, ²Zhejiang University City College, Hangzhou 310015, China, ³Biomedical Engineering, University of Connecticut, Storrs, CT 06269, USA, ⁴Electrical and Computer Engineering, University of Connecticut, Storrs, CT 06269, USA, ⁵Institute of Electromagnetic Fields (IEF), ETH Zurich, 8092 Zurich, Switzerland.

In Physics, causality is a fundamental postulation arising from the second law of thermodynamics. It states that, the cause of an event precedes its effect. In the context of Electromagnetics, the relativistic causality limits the upper bound of the velocity of information, which is carried by electromagnetic wave packets, to the speed of light in free space (c). In anomalously dispersive media (ADM), it has been shown that, wave packets appear to propagate with a superluminal or even negative group velocity. However, Sommerfeld and Brillouin pointed out that the “front” of such wave packets, known as the initial point of the Sommerfeld precursor, always travels at c . In this work, we investigate the negative-group-velocity transmission of half-sine wave packets. We experimentally observe the wave front and the distortion of modulated wave packets propagating with a negative group velocity in a passive artificial ADM in microwave regime. Different from previous literature on the propagation of superluminal Gaussian packets, strongly distorted sinusoidal packets with non-superluminal wave fronts were observed. This result agrees with Brillouin’s assertion, i.e., the severe distortion of seemingly superluminal wave packets makes the definition of group velocity physically meaningless in the anomalously dispersive region.

According to electromagnetic theory, material dispersion regulates the propagation of electromagnetic waves in a medium^{1–3}. With material dispersion, the wave velocity is no longer uniquely defined. This gives rise to the distinction between the phase, group and front velocities of electromagnetic waves⁴. The scientific community has recognized that the front velocity, rather than the group velocity, is the velocity that characterizes the transmission speed of information^{4–8}. However, confusions still exist: while the direct observation of the Sommerfeld precursor is very difficult due to its ultra-low signal-to-noise ratio (SNR)⁹, a number of experiments based on “fast-light” laser media have demonstrated seemingly non-distorted superluminal Gaussian pulses^{10–15}. It seems conflicting to have a non-superluminal wave front with a following non-distorted superluminal wave packet. In this paper, we use half-sine packets to observe the front edge of the waveform, which appears right after the Sommerfeld precursor. In this way, both the non-superluminal wave front and the superluminal, but strongly distorted wave packet can be directly measured.

Results

Transient analysis. A passive medium can be considered as a linear, time-invariant “system”. For a normalized plane wave transmitting in the z direction, the transfer function takes the form of $H(\omega) = e^{ik(\omega)z}$, where the complex wave number $k(\omega) = \alpha(\omega) + i\beta(\omega) = \omega\sqrt{\varepsilon(\omega)\mu(\omega)}$. The corresponding phase, group and front delays at distance z are

$$T_p = \frac{z}{v_p} = \frac{\alpha(\omega)}{\omega}z, T_g = \frac{z}{v_g} = \frac{d(\alpha(\omega))}{d\omega}z, T_f = \frac{z}{v_f} = \lim_{\omega \rightarrow \infty} \frac{\alpha(\omega)}{\omega}z \quad (1)$$

where v_p, v_g, v_f are the phase, group and front velocities, respectively¹⁶. For modulated wave packets, T_p, T_g and T_f represent the phase delays of the carrier, the envelope and the front end of the wave packets, respectively. Under such definitions, when ω approaches infinity, $\varepsilon(\omega)$ and $\mu(\omega)$ become ε_0 and μ_0^2 , and the front velocity v_f converges to speed of light in vacuum, c . It is well known that a single frequency waveform does not carry



useful information. Sommerfeld asserted that, v_f , the velocity of the front end of the transient perturbation before the rising edge, can be used to describe the traveling speed of information. On the other hand, since v_f always equals c , if the remaining part of the wave packet propagates with a superluminal or negative group delay, the continuous phase advancing of the wave packet would inevitably result in an envelope distortion.

Fig. 1a shows the classical Lorentz dispersion model of permittivity with a resonance frequency ω_0 . Within the frequency region marked in gray, this medium can be considered as an ADM. The propagation of Gaussian and half-sine packets within this anomalous region are shown in Fig. 1b and 1c, where point A is the location of the source and point B is the receiving point. For comparison, the same wave packets propagating in the air are also presented. We can see in Fig. 1b that, in the ADM, the Gaussian packet exits at the receiving point B without observable distortion before it comes out from the source point, while in the air, the opposite case is observed.

Due to the fact that the initial point of the rising edge of a Gaussian pulse extends to infinity with an extremely low SNR, the wave packet distortion is immersed by the noise at the place distant from the observable rising edge. However, for the half-sine packet employed in our setup, there are abrupt disturbances at both the initial and ending points (i.e. the two zero-crossing points), which immediately connect with the rising and falling edges. As a result, the non-superluminal front delay and the superluminal or negative group delay can be simultaneously measured. Induced by the superluminal group delay, the continuous phase advancing results in a “reshaping” of the envelope, so much that the half-sine envelope does not end at a zero-crossing (Fig. 1c). If such a distorted pulse is measured with a time-domain instrument (such as an oscilloscope), an additional “tail” as demonstrated in Fig. 1c can be observed due to the transient discharge response.

It is worth noting that the two abrupt disturbances (starting and ending points of the half-sine packet) both propagate at c , and therefore the length of the half-sine packet (T) is equal to that in the air. In such a case, we can see the strong distortion at the rising and falling edges due to the forward reshaping effect, which preserves the relativistic causality.

Full wave simulation. In our previous work¹⁷, we have verified that, at the vicinity of the plasma frequency, an effective uniaxial medium consisting of periodically arranged split-ring resonators exhibits an anomalous dispersion for oblique incidence due to a special k-surface distortion. In this frequency region, a maximum negative group velocity of $-0.3c$ was experimentally measured with a continuously modulated sinusoidal packet. In this work, instead, we observe the discrete sinusoidal signals consisting of half-sine packets propagating in the same effective medium.

The inset of Fig. 2a shows the simulation model we used in reference 17, where the permeability of the uniaxial medium along the z axis follows a Drude model. As discussed, such an uniaxial medium can be considered with a scalar permittivity $\epsilon_r = 1$ and a permeability tensor $\mu_r = \text{diag}(1, 1, \mu_{rz})$, where $\mu_{rz} = 1 - \omega_p^2/[\omega(\omega + i\gamma_e)]$, $\omega_p = 10$ GHz and $\gamma_e = 0.02\omega_p$. With an oblique incidence polarized along the y direction, the k-surface of the medium is

$$k_x^2/\mu_{rz} + k_z^2 = \epsilon_r k_0^2 = \epsilon_r (\omega/c)^2 \quad (2)$$

where k_0 is the wave number in air, k_x and k_z are the wave numbers in the x and z directions, respectively. Due to the k-surface distortion occurring at the plasma frequency as an effect of inevitable loss and the oblique incidence, an anomalous dispersion of k_z ranging from $0.993\omega_p$ to $1.022\omega_p$ appears at the vicinity of the plasma frequency¹⁷, as shown in Fig. 2a.

Using a commercial Maxwell equations solver, CST microwave studio (<https://www.cst.com/Products/CSTMWS>), we simulated the propagation of half-sine packets in the ADM. Fig. 2b shows the propagation of modulated wave packets representing binary series of “1”s and “0”s in the air and a 20-cm-thick sample. The incident angle was chosen to be 10 degree. Two probes were placed along the z direction, at point A ($z = 20$ mm) and point B ($z = 140$ mm), to detect the wave packets in real time.

First, a 10-GHz carrier modulated with a 12.5-ns half-sine envelope (representing information symbol “1”) following a 7.5-ns zero-volt duration (representing information symbol “0”) is chosen to serve as the incident packets. The wave packets detected at points A and B, as well as the incident packets, are shown in the left panel of Fig. 2b. For comparison, we also performed a reference simulation with the same configurations except a carrier frequency of 12 GHz (out of the anomalous dispersion region), and the results are shown in the right panel of Fig. 2b. In both panels of Fig. 2b, the incident packets are used as reference, whose amplitudes have an arbitrary unit. However, for the wave packets detected inside the medium, their amplitudes are normalized to the amplitudes detected at point A. We can see that, for the case of anomalous dispersion, the wave packet propagates with large attenuation and severe distortion. In contrast, for the normal dispersion case, the wave packets propagate inside the uniaxial medium without notable distortion. This result complies with the prior knowledge of the dispersion characteristic of the uniaxial medium.

The envelopes of above wave packets shown in Fig. 2b are further extracted and plotted in the panel (I) (anomalous dispersion case) and panel (II) (normal dispersion case) of Fig. 2c, correspondingly. It is worth to discuss the differences between these two cases. First, the front-end point (where information symbol changes from “0” to “1”) of each envelope travels from point A to point B with the same front

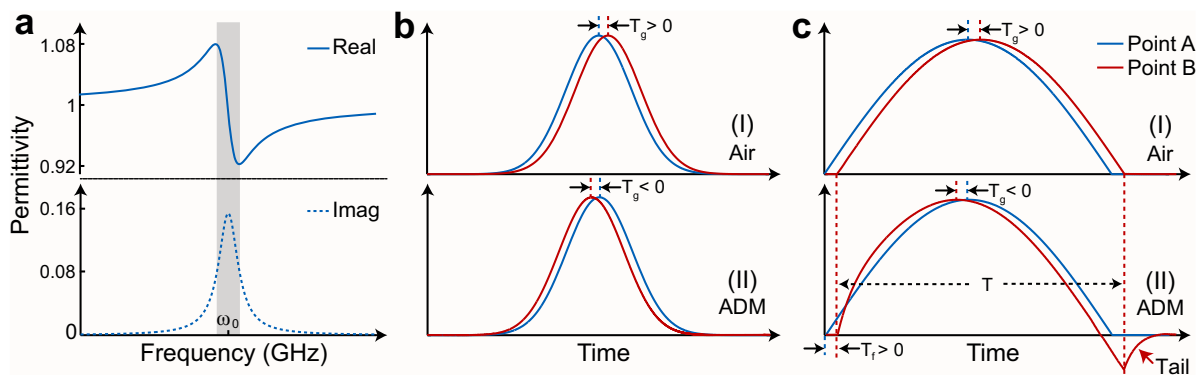


Figure 1 | Theoretical analysis. (a) Real and imaginary parts of the permittivity of a Lorentzian medium with a resonance frequency of ω_0 . In the gray region, this medium can be considered as an ADM. (b) The demodulated Gaussian packets propagating in the air and in the ADM. (c) The demodulated half-sine wave packets propagating in the air and in the ADM. Point A is the location of the source and point B is the receiving point.

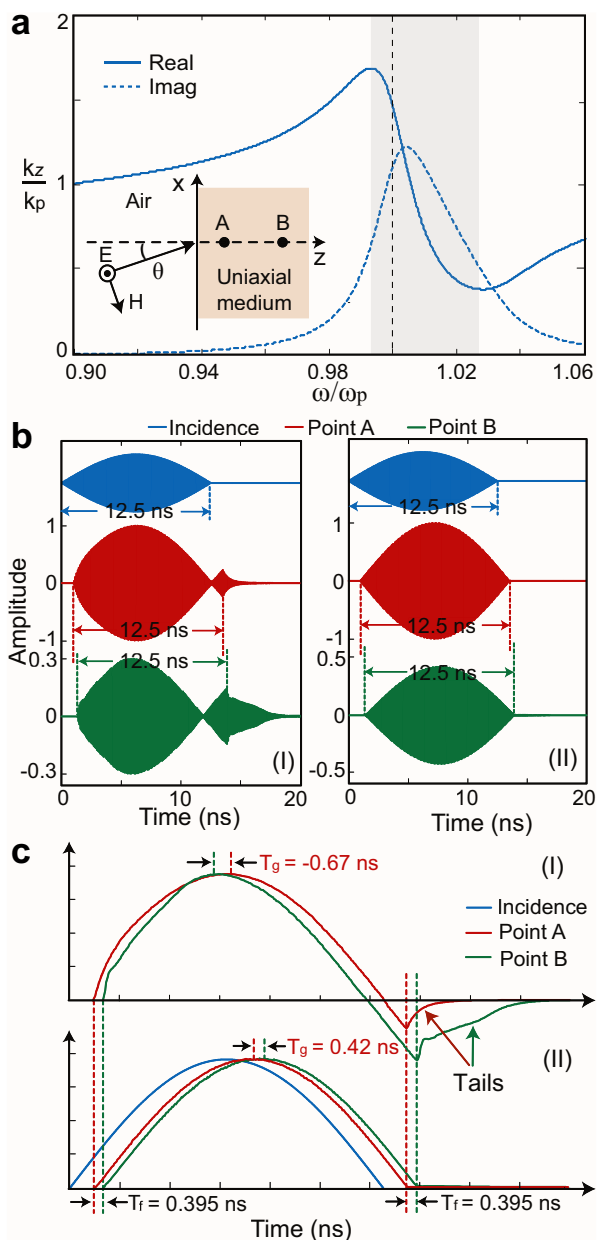


Figure 2 | Theoretical and Simulated results. (a) The wave vector k along z axis around the plasma frequency at an oblique incidence (10°), where the inset shows the diagram of EM wave packets impinge on the surface of a uniaxial plasma medium. (b) Full wave simulation of half-sine wave packets propagating in the uniaxial plasma medium with $\omega_p = 10$ GHz and $\gamma_e = 0.02\omega_p$, at anomalous (Panel I), carrier frequency of 10 GHz) and normal (Panel II), carrier frequency of 12 GHz) dispersion regions, where the incident angle is 10° . (c) Normalized envelopes of half-sine pulses.

delay $T_f = 0.395$ ns. Based on the incident angle (10 degrees) and the front delay, v_f can be calculated to be 2.99×10^8 m/s, which is very close to c . We see that v_f is positive and non-superluminal, in accord with the definition of Eq. (1). We note that, when information symbol changes from “1” to “0”, the discontinuous responses have the same delay, i.e. 0.395 ns. This implies that the consecutively transmitted wave packets, either “1”s or “0”s, have the same front velocity. Second, the group delay T_g in the panel (I) of Fig. 2c is negative 0.67 ns, while in the panel (II), it is positive 0.42 ns. Compared with the incident envelope, the peak of the transmitting envelope arrives at point B prior to A, indicating an apparent negative group velocity.

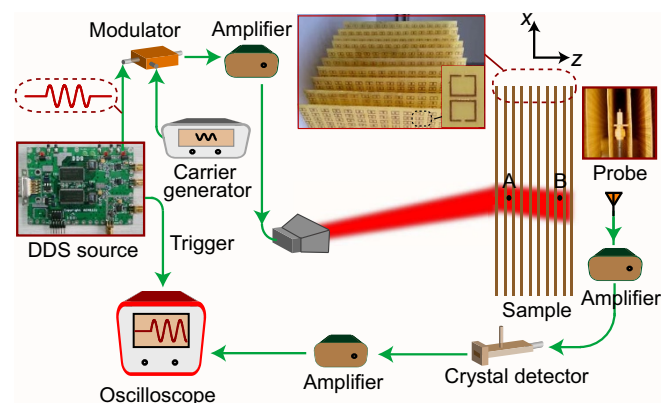


Figure 3 | Experimental setup.

Lastly, due to the negative group delay, the continuous phase advancing of the packet reshapes the envelope. It is seen that both at point A and B, the half-sine envelopes do not end at a zero-crossing. Instead, the envelope ends beyond the zero-crossing to conserve the pulse length, and the “tail” also appears as expected, in Fig. 2c. These full-wave simulations are in a good agreement with previous analysis.

As indicated in Fig. 2b and 2c, the sustained phase advancing causes the original half-sine envelope to be strongly distorted, producing a fish-like envelope with an extra “tail”. This strongly distorted envelope implies that the negative group velocity is an envelope reshaping due to a strong anomalous dispersion. To this end, the definition of negative group velocity in an anomalously dispersive region is no longer meaningful from the wave velocity point of view, as it actually describes the degree of envelope reshaping rather than the transmission velocity of information.

Experimental validation. Experimental measurements have been performed to validate aforementioned analyses and simulations. In the measurement, different from previous analysis and simulation, a three-cycle sinusoidal signal consisting of six half-sine packets with length $T = 300$ ns is repeatedly generated in a cycle of 0.1 microseconds using a direct digital synthesis (DDS) source¹⁸, to serve as the modulation envelope. By using 6 continuous half-sine waveforms, we can easily compare the lengths of the first and last half-sine envelopes with those of the middle ones, and as such, we can accurately determine the starting and ending locations of the strongly distorted envelopes.

The experimental setup is shown in Fig. 3. The slab-like sample consists of ten layers of printed circuit boards carrying periodically arranged sub-wavelength split-ring resonators¹⁹. The dispersion of the effective z -component permeability closely follows a typical Lorentzian dispersion model with a typical plasma dispersion region between 9.35 GHz and 9.65 GHz, with $\omega_p \approx 9.45$ GHz and $\gamma_e \approx 0.05\omega_p$ ¹⁷. A 9.5-GHz carrier is provided by a microwave source (Agilent’s E8257D), which is modulated by the envelope signal with a modulation module (Seekon microwave’s XKMIX20180). The envelope signal is triggered by rectangular pulses generated by an arbitrary waveform generator (Agilent’s 33210A), which is simultaneously used as the trigger signal for the oscilloscope, to synchronize the demodulated envelope detected by the receiver. The modulated carrier is amplified by a microwave amplifier (Agilent’s XKLA8018N3520-61), and then sent to a transmitting horn antenna (HD microwave’s HD-100HA20) located 1.5 meters away from the sample.

By rotating the horn antenna, the modulated carrier leaving the antenna is adjusted to be electrically polarized along the y direction, and impinges on the surface of the sample with an incident angle of 15 degrees. Inside the sample, we place the probe (a monopole antenna) at points A and B, separately, to measure the intensity of



the wave packets. The detected signal is amplified by a low noise amplifier (Seekon Microwave's XKLA8018N3520-6L), then demodulated by a crystal detector (Yamei Microwave's BO-20A) to recover the envelope and finally amplified by a low frequency amplifier (Sonoma Instrument's 310). Synchronized by the trigger signal, the demodulated envelope is displayed and sampled using a high sampling rate digital oscilloscope (Tektronix's MSO 4104B). Since both the DDS source and the oscilloscope have been synchronized by the high-quality trigger pulses provided by the Agilent's 33210A, the envelope captured by the MSO 4104B is able to provide definite time delay with respect to the trigger signal.

Finally, the measured waveform is downloaded from the MSO 4104B, based on which the demodulated envelope can be numerically processed, and the front and group delays can be calculated. In order to remove random noises, a digital 3rd-order Butterworth low-pass filter is used to filter the measured raw data, and standard deviation is calculated to estimate the error of the measuring points.

The demodulated envelopes, with a carrier frequency of 9.5 GHz, were directly obtained, as shown in Fig. 4a. It is shown that the amplitude of the envelope decays as the wave propagates in the sample from point A to point B (the interval between them is 9.6 cm) with a strong attenuation, which makes sense according to the condition of anomalous dispersion. It is seen that except for the first zero-crossing, the subsequent zero-crossings (as well as the peaks) of the envelope are firstly seen at the further point B, and they propagate backwards to point A (2.9 ± 0.2 ns later) as shown in the panel (II) of Fig. 4b, corresponding to an average negative group velocity around $-0.11c$.

In the panel (I) of Fig. 4b, we show the first rising edge detected at points A and B with normalized amplitudes. It is seen that the "front" of the packet, located before 60 ns, is firstly seen at point A, propagating forward to point B, which agrees with the simulated results shown in the Fig. 2b–c. The measured front delay is about 0.36 ± 0.2 ns, corresponding to an average front velocity $v_f \approx 0.86c$. This is in accordance with the theoretical expectation. In the meantime, we observe in Fig. 4a that at both points A and B, the last half-sine packet does not end at the zero-cross indicated by the ideal non-distorted envelop (the dash green line), and the "tails" are clearly captured by the oscilloscope. It is also observable that at the further point B, the "tail" gets visibly larger, further validating the simulated analysis.

Finally, it is worth noting that in the six consecutive half-sine packages, the observable strong distortion occurs at the first and

the last half-sine packages. Distant from the starting and ending points where symbols change between "1"s and "0"s, the other four half-sine waveforms in the middle are not notably distorted. This is what happened to the superluminal optical Gaussian packets reported in previous literature.

Discussion

In conclusion, we have demonstrated an unusual travelling of electromagnetic wave packets with a negative group velocity and a non-superluminal positive front velocity, in both simulation and experiment. Different from previous literature on superluminal optical Gaussian packets without notable distortion, the strongly distorted discrete half-sine packets with a non-superluminal wave front was observed in our experimental setting. The reported result validates Brillouin's assertion that in the wave velocity point of view, the distortion of seemingly superluminal wave packets makes the definition of group velocity a physically meaningless concept in the anomalously dispersive region, where the negative group velocity can also be understood as the description of how fast the envelope is reshaped. Such a causal pulse propagation and distortion prevent a violation of the relativistic causality, and can be used to interpret the causality issues of superluminal transmission of electromagnetic waves in all kinds of ADM and gain media.

We also note that, a recent work used a "compact-support pulse" in a negative-group-delay circuit to observe the phenomena like steepening and shock-like waves²⁰. Our results, on the other hand, used a three-dimensional space experiment to verify that, the non-analytical point (in our paper the point with "abrupt disturbance") in the pulse's leading edge propagates at the velocity of light in vacuum. Our results also explicitly answered the uncertainty raised in Ref. 20, i.e., whether the non-analytical point of trailing-edge can be associated to information as the same way as the leading-edge.

Based on our analysis, simulation and experimental results, our conclusion is that the non-analytical point of trailing-edge also travels at speed c , the same as the non-analytical point of leading edge. The fact supporting our conclusion is that the change of information symbols from '1' to '0' and from '0' to '1' plays the same role in the wave package transmission, because both of them carry information.

In our simulation and measurement, the length of the distorted pulse between two successive non-analytical points is equal to that of the incident pulse. We have observed that, the forward "re-shaping" effect by the continuous phase advancing results in a severe wave packet distortion, and the pulse does not end at a zero-crossing point. As such, the induced "tail" due to the transient discharge response is not a part of the severely distorted wave packet. Instead, the "tail" begins at the ending point of the packet. This observation is consistent with Sommerfeld's theory.

Methods

Fabrication of the experimental sample. The slab-like experimental sample consists of multilayer printed circuit boards (PCBs) carrying sub-wavelength split-ring resonators (SRRs). In the fabrication process, the metallic (copper) SRRs were printed on 0.5-mm-thick FR4 substrates, with a relative permittivity around 4.6 at microwave frequencies. Each board contains 82 unit cells along the x direction with a periodicity of 6 mm and 15 unit cells in the y direction with a periodicity of 10 mm. Eleven layers of such PCBs were aligned along the z direction spaced by 16 mm to form a slab-shaped sample with a width of 500 mm along the x direction, 150 mm in the y direction and a thickness of 160 mm in the z direction.

For an oblique incident wave with the electric field polarized in the y direction impinging upon such a medium, magnetic resonances can be induced at the metallic rings, yielding a strong dispersion of permeability with a negative band of μ_{rz} ^{17,19}. Meanwhile, there is no magnetic response in x and y directions, and thus μ_{rx} and μ_{ry} can be treated as unity. In our previous work¹⁷, we have validated that the dispersion of μ_{rz} follows a classical Drude-Lorentz dispersion model with a plasma frequency of around 9.45 GHz and there exists an anomalous dispersion region between 9.45 GHz and 9.55 GHz with a 15-degree incident angle.

1. Kong, J. A. *Electromagnetic wave theory* (EMW Pub.: Cambridge, 2000).

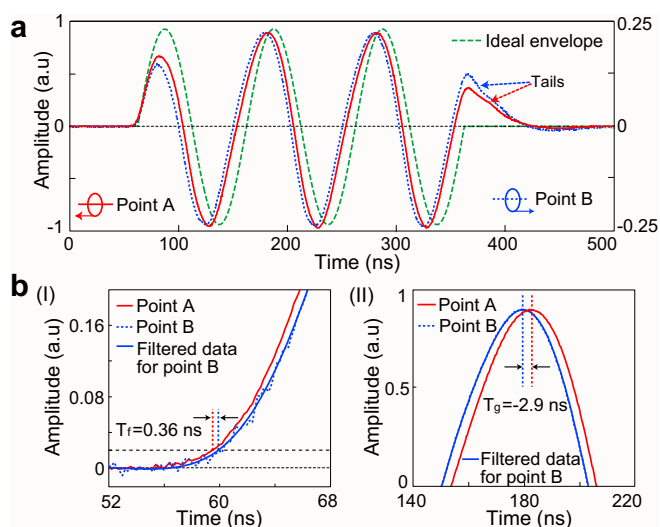


Figure 4 | Measured results. (a) The experimental demodulated envelopes in time domain measured at points A and B, where the carrier frequency is 9.5 GHz. (b) Detailed views of the first rising edges with normalized amplitudes for the panel (I) and the second peaks of envelopes for the panel (II).



2. Milonni, P. W. *Fast light, slow light and left-handed light* (Institute of Physics: Bristol, 2005).
3. Jackson, J. D. *Classical electrodynamics* (Wiley: New York, 1999).
4. Brillouin, L. *Wave propagation and group velocity* (Academic Press: New York, 1960).
5. Gehring, G. M., Schweinsberg, A., Barsi, C., Kostinski, N. & Boyd, R. W. Observation of backward pulse propagation through a medium with a negative group velocity. *Science* **312**, 895–897 (2006).
6. Sommerfeld, A. The propagation of light in dispersing media. *Ann. Phys-Berlin* **44**, 177–202 (1914).
7. Stenner, M. D., Gauthier, D. J. & Neifeld, M. A. The speed of information in a ‘fast-light’ optical medium. *Nature* **425**, 695–698 (2003).
8. Brillouin, L. On the propagation of light in dispersing media. *Ann. Phys-Berlin* **44**, 203–240 (1914).
9. Bolda, E. L., Garrison, J. C. & Chiao, R. Y. Optical pulse-propagation at negative group velocities due to a nearby gain line. *Phys. Rev. A* **49**, 2938 (1994).
10. Dolling, G., Enkrich, C., Wegener, M., Soukoulis, C. M. & Linden, S. Simultaneous negative phase and group velocity of light in a metamaterial. *Science* **312**, 892–894 (2006).
11. Li, L., Guo, H., Xiao, F., Peng, X. & Chen, X. Z. The control of superluminal group velocity in a system equivalent to the Y-type four-level atomic system. *Phys. Lett. A* **334**, 214 (2005).
12. Zhang, L. *et al.* Superluminal propagation at negative group velocity in optical fibers based on Brillouin lasing oscillation. *Phys. Rev. Lett.* **107**, 093903 (2011).
13. Wang, L., Kuzmich, A. & Dogariu, A. Gain-assisted superluminal light propagation. *Nature* **406**, 277–279 (2000).
14. Deng, D. *et al.* Negative group velocity propagation in a highly nonlinear fiber embedded in a stimulated Brillouin scattering laser ring cavity. *Appl. Phys. Lett.* **103**, 251110 (2013).
15. Garrett, C. G. B. & Mccumber, D. E. Propagation Of a Gaussian Light Pulse Through an Anomalous Dispersion Medium. *Phys. Rev. A* **1**, 305 (1970).
16. Papoulis, A. *The Fourier Integral and its Applications* (McGraw-Hill, Inc.: New York, 1962).
17. Ye, D. *et al.* Negative group velocity in the absence of absorption resonance. *Sci. Rep.* **3**, 1628 (2013).
18. Gu, C., Qiao, S., Huangfu, J. & Ran, L. DDS Based radar signal generator for microwave remote sensing. *Proc. Progress. Electromagn. Res. Symp.* **3**, 40–43 (2008).
19. Ye, D., Qiao, S., Huangfu, J. & Ran, L. Experimental characterization of the dispersive behavior in a uniaxial metamaterial around plasma frequency. *Opt. Express* **18**, 22631 (2010).
20. Hickmann, J. M., Alencar, M. A. R. C., Silva, W. F. & Souza, S. T. Causality-induced pulse steepening and shock-like waves in superluminal media. *Epl-Europhys. Lett.* **97**, 44009 (2012).

Acknowledgments

This work was supported by the NSFC under grants 61102003, 61131002 and 61401393, the China Postdoctoral Science Foundation under grant 2014M550325, and the China CAST foundation under grant 201321.

Author contributions

D.Y., Y.S. and L.R. designed the research; D.Y., Y.S., J.H., S.Q. and G.Z. performed the research; S.Q. supervised the research. All authors contributed to data interpretation and the composition of the manuscript.

Additional information

Competing financial interests: The authors declare no competing financial interests.

How to cite this article: Ye, D. *et al.* Observation of Wave Packet Distortion during a Negative-Group-Velocity Transmission. *Sci. Rep.* **5**, 8100; DOI:10.1038/srep08100 (2015).



This work is licensed under a Creative Commons Attribution-NonCommercial-NoDerivs 4.0 International License. The images or other third party material in this article are included in the article's Creative Commons license, unless indicated otherwise in the credit line; if the material is not included under the Creative Commons license, users will need to obtain permission from the license holder in order to reproduce the material. To view a copy of this license, visit <http://creativecommons.org/licenses/by-nc-nd/4.0/>